

Twisted Bilayer Graphene Aligned with Hexagonal Boron Nitride: Anomalous Hall Effect and a Lattice Model

Ya-Hui Zhang, Dan Mao, and T. Senthil

Department of Physics, Massachusetts Institute of Technology, Cambridge, MA, USA
(Dated: January 25, 2019)

A recent experiment reported a large anomalous Hall effect in Magic Angle Twisted Bilayer Graphene (TBG) aligned with a hexagonal boron nitride (h-BN) substrate at $\frac{3}{4}$ filling of the conduction band. In this paper we study this system theoretically, and propose explanations of this observation. We emphasize that the physics for this new system is qualitatively different from the pure TBG system. The aligned h-BN breaks in-plane two-fold rotation symmetry and gaps out the Dirac crossings of ordinary TBG. The resulting valence and conduction bands of each valley carry equal and opposite Chern numbers $C = \pm 1$. A useful framework is provided by a lattice extended Hubbard model for this system which we derive. An obvious possible explanation of the anomalous Hall effect is that at $3/4$ -filling the system is a spin-valley polarized ferromagnetic insulator where the electrons completely fill a Chern band. We also examine an alternate more radical proposal of a compressible valley polarized but spin unpolarized composite fermi liquid metallic state. We argue that either state is compatible with current experiments, and propose ways to distinguish between them in the future. We also briefly discuss the physics at $1/2$ filling.

Moiré superlattices from twisted Van der Waals heterostructures have emerged as promising platforms to study strongly correlated effects with high tunability [1–5]. Correlated insulators and superconductors have been found in twisted bilayer graphene and ABC stacked trilayer graphene/hexagonal boron nitride (TG/h-BN) [2–5].

Very recently a large anomalous Hall effect was observed [6] in Magic Angle-Twisted Bilayer Graphene (MA TBG) at conduction band filling $\nu = \frac{3}{4}$. Specifically hysteretic jumps in both the Hall resistivity (ρ_{xy}) and longitudinal resistivities (ρ_{xx}) were observed. At the lowest temperatures, $\rho_{xy} \approx 0.5 \frac{h}{e^2}$ and $\rho_{xx} \approx 0.3 \frac{h}{e^2}$, corresponding to a large Hall angle, are measured. Evidence for non-local transport, indicative of conducting channels at the sample edge, have been presented. A key new feature of the device studied in Ref. 6 is that one of the graphene layers is nearly aligned with a hexagonal-Boron Nitride (h-BN) substrate. This alignment has many important effects, as we explain below, and serves to distinguish this system from previous experiments on Magic Angle TBG where no such anomalous Hall effect has been reported.

In this paper we study theoretically the MA TBG-hBN system, and propose possible explanations of these observations. A spontaneously spin-valley polarized Chern insulator at $3/4$ filling provides a simple and natural explanation for the large anomalous Hall effect. We also consider a different novel state which may also explain the data - a compressible composite fermi liquid metal with valley polarization but no spin polarization. We propose experiments to distinguish these two distinct states.

In the absence of alignment with h-BN, the moiré bandstructure of MA-TBG has “active” nearly flat bands that are well separated from other bands. The active bands live in each of two Mini Brillouin Zones (MBZ) cor-

responding to the two valleys of the underlying graphene layers. Within each valley the conduction and valence active bands are connected by Dirac points at the corners of the MBZ. These Dirac points are protected by an excellent emergent C_2T symmetry where C_2 refers to a 2-fold rotation and T is time reversal. Either C_2 or T maps one valley to the other but their combination preserves the valley index. If however C_2T is broken then the Dirac points will become gapped. Experimentally the presence of Dirac points is evidenced by studying the properties of the system filled to the Charge Neutrality Point (CNP). Typically at CNP the system is metallic with a low but non-zero conductance.

An important effect of alignment with h-BN is that the broken C_2 symmetry of h-BN is transmitted to the graphene bands. Thus the Dirac points are gapped and insulating behavior may obtain at CNP. This is supported by the measured ρ_{xx} at neutrality in Ref. 6 which is much bigger than the typical measured values in unaligned TBG devices. Furthermore the resulting isolated conduction and valence bands in each valley carry Chern numbers $C = 1, -1$ (opposite valleys carry opposite Chern numbers). Thus the MA TBG-hBN is similar to the many other examples of nearly flat $\pm C$ bands discussed theoretically recently [7]. As emphasized in Ref. 7, at total fillings $\nu_T = 1, 3$ nearly flat \pm Chern bands are an excellent platform for the quantum anomalous Hall effect, as well as other even more novel many body states. Recently Ref. 8 described a spin-valley polarized quantum anomalous Hall state in unaligned twisted bilayer graphene where C_2T is broken by interaction effects.

A further effect of the alignment with h-BN is that there are now two distinct moiré superlattices. In addition to the moiré potential produced by the relative twisting of the two graphene layers, the lattice mismatch

between h-BN and graphene produces another moiré potential[9]. These two moiré lattices have roughly the same period but are rotated by 90° relative to each other which makes them mutually incommensurate. However the strength of the h-BN induced moiré potential is expected to be weaker than the other one, and it is a reasonable approximation to ignore it to begin with. It may however play a role by producing in-gap states that may contribute to the lack of exact quantization of the Hall resistivity (in addition to other mechanisms involving disorder) in the experiments.

The experimental developments on correlated moire superlattices has spawned a large theoretical literature - for a sample see Refs. 10–51. An important conclusion[11, 35, 36, 47, 48] is that the bands of TBG have (symmetry) protected topological structure which obstruct the construction of lattice tightbinding models with natural (“on-site”) action of all symmetries. The C_2T breaking induced by the alignment with h-BN however removes this obstruction, and it is possible to construct a lattice tightbinding model to represent the conduction and valence band taken together within each valley. Unsurprisingly, we show that this takes the form of a lattice Haldane model. Combining the 2 valleys and projecting the Coulomb interaction yields an effective lattice ‘extended’ Hubbard model suitable for TBG-hBN. This lattice model provides a useful framework to discuss the physics and may also be useful for future numerical studies.

We consider twisted bilayer graphene where the top layer is aligned with the h-BN layer substrate. The twist angle between the two graphene layers θ_M is chosen to be close to the magic angle $\theta_M = 1.05^\circ - 1.20^\circ$. The twist angle between the top h-BN layer and the top graphene layer θ_{hBN} is close to zero. We assume the bottom h-BN substrate is misaligned and its effect can be ignored.

We use the standard continuum model[52] (with $\frac{w_0}{w_1} = 0.7$ [12] to account for lattice relaxation) to calculate the band structure of the TBG/h-BN system. As time reversal symmetry flips the valley, we can focus only on the band structure within a single valley, say +. The Hamiltonian is

$$H = H_{TBG} + H_{hBN} \quad (1)$$

Here H_{TBG} is the continuum model for the TBG in Ref. 52. The aligned h-BN has two effects on the top graphene layer:

$$H_{hBN} = \sum_{\mathbf{k}} M \psi_t^\dagger \mu_z \psi_t + \sum_{j=1,\dots,6} \psi_t^\dagger(\mathbf{k} + \mathbf{Q}'_j) V_j \psi_t(\mathbf{k}) \quad (2)$$

where $\psi_{t,b}$ represent electron destruction operators in the top and bottom valley. The first term is an induced staggered potential on the A, B sublattices of the top graphene layer which acts as a ‘mass’ term. A rough estimate is obtained from experiments on monolayer graphene nearly aligned with h-BN which show that

the band gap at the neutrality point is around 35 meV. This implies $M \approx 17$ meV. The second term in Eq. 2 represents the moiré potential coming from the lattice mismatch between h-BN and graphene. The resulting moiré wavevectors are *incommensurate* with those associated with the TBG superlattice. Furthermore a rough estimate from DFT calculations gives $V_j \approx 10$ meV[9] which is much smaller than the strength of the TBG moiré term (around 110 meV[52]), and somewhat smaller than the first term. Thus as a first approximation we ignore the V_j . This considerably simplifies our analysis as we now have a well defined band structure in the moiré superlattice of TBG.

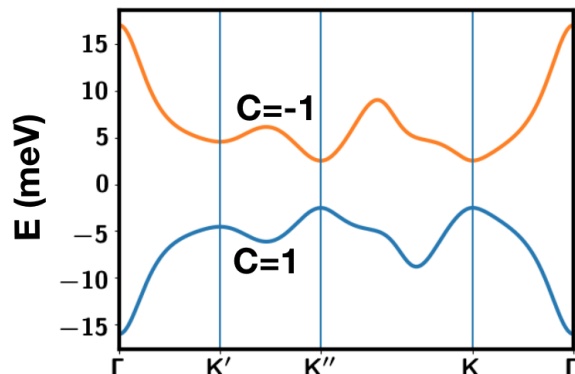


FIG. 1: Band structure for valley + of the TBG/h-BN system in the MBZ. $\theta_M = 1.20^\circ$. The band of valley - can be generated from the time reversal transformation.

The band structure is shown in Fig. 1 for $M = 15$ meV. As expected, there is a finite band gap around 5 meV for the value of M we used. Importantly through explicit calculation the conduction and the valence bands for the valley + has Chern number $C = 1, -1$. This Chern number is a simple symptom of the underlying subtle band topology[11, 35, 36, 47, 48] of the unaligned TBG system, and is closely related to the ‘flipped Haldane model’ picture described in Ref. 35.

In addition to the Berry curvature, the massive Dirac cone at K or K' point with gap Δ have an out-of-plane orbital magnetic moment proportional to $\frac{1}{\Delta}$ [53]. As a result, there is a valley Zeeman coupling $-g_v \mu_B H_z \frac{\tau_z}{2}$ to the magnetic field in the z direction, where $\tau_a, a = x, y, z$ is the Pauli matrix in valley space. We numerically calculated g_v for $\theta_M = 1.20^\circ$ and $M = 15$ meV. Indeed we find that close to the K and K' point, $g_v(K) \approx g_v(K') \approx 15$ for both conduction and valence bands, much larger than the spin Zeeman coupling. At neutrality point, this large valley Zeeman coupling can cause splitting between the two valleys in an out of plane magnetic field. This ex-

plains the two fold degeneracy of the Landau fan observed near charge neutrality in Ref. 6.

Combining the two valleys, we can now project the Coulomb interaction on to these bands to obtain an effective model. There are three important energy scales: the bandwidth W of the conduction band, the band gap Δ (between conduction and valence bands) and the interaction strength U . Our focus is on the experimentally observed correlated insulators at $\nu = 1/2$ and $\nu = 3/4$ of the conduction band.

First consider the limit $\Delta \gg U \gg W$. Then we only need to keep the four conduction bands (including spin and valley) and the problem reduces to the nearly flat \pm Chern band system studied in Ref. 7. In the flat band limit, the ground state should be a ferromagnetic insulator from spin or valley polarization. In particular valley polarization is favored over intervalley coherence within a Hartree-Fock calculation[7]. For $\nu = \frac{3}{4}$, quantum anomalous Hall effect(QAHE) with $|\sigma_{xy}| = \frac{e^2}{h}$ emerges by polarizing both spin and valley. At $\nu = \frac{1}{2}$ in this flat band limit, we expect instead a spin polarized insulator with a quantum valley Hall effect.

Strictly speaking, the TBG/h-BN system is in a different limit $U \sim W > \Delta$ and the detailed many body physics may differ from that discussed in Ref. 7. When $\Delta < W$, both the conduction bands and the valence bands should be kept in the low energy model. Below we provide a lattice model by Wannier construction of the active bands which, in contrast to standard TBG, is possible given the broken C_2T symmetry. The system still has a C_3 rotation symmetry. We take the rotation center as the AA site. The C_3 eigenvalues at Γ, K, K' are $1, \omega, \omega$ for the conduction band and $1, \omega^*, \omega^*$ for the valence band, with $\omega = e^{i\frac{2\pi}{3}}$. The distinct eigenvalues at Γ, K, K' implies that we cannot represent the system on the natural triangular lattice formed by the AA regions. A honeycomb representation is however possible. The corresponding Wannier functions are readily constructed and have the familiar fidget-spinner shape[11] reflecting the concentration of charge in the AA regions.

Let $\mathbf{a}_1 = a_M(0, 1)$ and $\mathbf{a}_2 = a_M(\frac{\sqrt{3}}{2}, \frac{1}{2})$ be two basis vectors for the honeycomb lattice, and define the electron operator $c_{i;a\sigma}$ where $a = \pm$ and $\sigma = \uparrow, \downarrow$ are the valley and spin index. The tight binding model takes the form

$$H_K = -m_0 \sum_i (-1)^{X(i)} c_{i;a\sigma}^\dagger c_{i;a\sigma} - \sum_{a\sigma} \sum_{ij} (t_{ij}^a c_{i;a\sigma}^\dagger c_{j;a\sigma} + h.c.) \quad (3)$$

where $X(i) = \pm 1$ on the A and B sublattices. Time reversal symmetry requires that $t_{ij}^\dagger = t_{ij}^{*} = t_{ij}$. For each valley this is a modified Haldane model in its topological phase (with a few extra hopping parameters). The tight binding parameters can be found in the supplementary.

The fidget spinner Wannier orbital implies that the interaction is dominated by a cluster charging[11] Hubbard interaction. Furthermore due to the the non-zero spatial

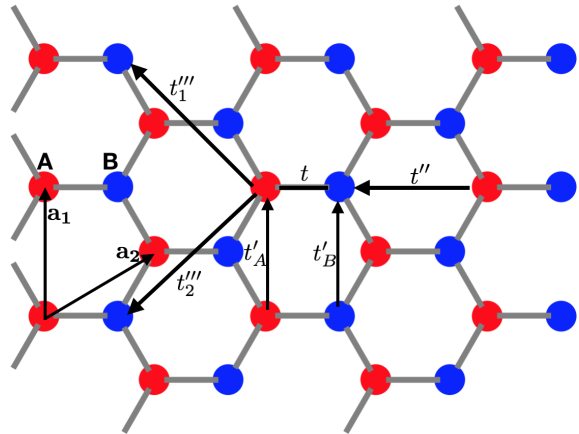


FIG. 2: Illustration of the lattice model on a Honeycomb lattice. $C_3 t(\mathbf{R}) C_3^{-1} = t(C_3 \mathbf{R})$ generates inter-sublattice hopping and $C_6 t'(\mathbf{R}) C^{-1}(6) = t'(C_6 \mathbf{R})$ generates intra-sublattice hoppings.

overlap between Wannier orbitals on different sites, there will be an inter-site Hund's term J [54, 55],

The interaction term is thus

$$H_V = U \sum_{\square} n_{\square}^2 - J \sum_{ij} \sum_p S_i^p S_j^p + \dots \quad (4)$$

Here n_{\square} is the electron charge summed over the sites of a hexagonal cluster. $p = 1, \dots, 15$ is summed over the 15 generators of $SU(4)$, and the ellipses represent other terms (eg a pair hopping) that are less important in the insulator.

Finally we have a lattice model by combining the kinetic and the interaction terms (Eqns. 3 and 4). Strictly speaking we also need to add a quasi-periodic potential from the incommensurate h-BN layer (see details in the supplementary).

Given this lattice model, we can consider the strong coupling limit $U \gg \Delta, W$. Then at integer total fillings we will get Mott insulators where the charge on every cluster is frozen. The corresponding insulator cannot have any Hall response: for a non-zero σ_{xy} , a Laughlin type of threaded flux induces charge $Q = \sigma_{xy} e$, while in the $U \gg \Delta, W$ limit the local density cannot be changed. Of course the experimental system is likely in the regime $U \sim W \gg \Delta$ and this strong coupling limit is not directly relevant.

The observation of a hysteretic anomalous Hall effect in the experiment[6] clearly shows[56] that there is spontaneous time reversal breaking associated with valley polarization at $\nu = \frac{3}{4}$. Assuming full valley polarization we then have a spinful "Haldane model" supplemented with interactions at half filling of the conduction band.

If the ground state is fully spin and valley polarized

then we get the Chern insulator, and there will be a quantized anomalous Hall effect. In an ideal sample, this state has $\rho_{xy} = \pm \frac{h}{e^2}$, $\rho_{xx} = 0$ corresponding to a Hall angle of 90° . Such a spin-valley ferromagnetic insulator state has very good Coulomb energy but has poor kinetic energy. Thus when $W \sim U$ it is interesting to contemplate other states of matter. We will assume full valley polarization in the discussion below.

For $W \gg U$ a simple Fermi liquid will be the ground state. This state has $\sigma_{xx} \gg e^2/h$, $\sigma_{xy} \sim e^2/h$. The Hall conductance is due to a quasiparticle Berry phase that will exist at generic filling of the Chern band. It follows that $\rho_{xy} \ll \rho_{xx}$ so that the anomalous Hall resistivity is small, unlike in the experiments.

How should we connect the Fermi liquid at $W \gg U$ to the ferromagnetic Chern insulator? A natural possibility (accessed through a Stoner mean field theory) is that the Fermi liquid first undergoes a transition to a partially spin polarized Fermi liquid which then gives way at larger interaction strengths to the fully spin polarized ferromagnetic insulator. The properties of the partially spin polarized metal will interpolate continuously between those of the spin unpolarized Fermi liquid and the ferromagnetic insulator. A key experimental signature of this phase will be the presence of two distinct oscillation frequencies (corresponding to the spin split Fermi surfaces) in Shubnikov-DeHaas (SdH) experiments.

We now describe a novel alternate possibility for an intermediate coupling phase. We reason by analogy to a Landau level to which a $C = 1$ band is closely analogous. Since each spin species is at half-filling of the $C = 1$ band, we may expect the system to be similar to that of spinful electrons in a half-filled Landau level. In the traditional half-filled Landau level it is well known that a compressible metallic state - the Composite Fermi Liquid (CFL) - is formed. In the presence of spin it is favorable to instead spin polarize to form a ferromagnetic integer quantum hall state. In contrast to the traditional Landau level, the Chern band has a dispersion. Thus a spin unpolarized Composite Fermi Liquid may be competitive. Such a state should retain much of the kinetic energy of the simple Fermi liquid while doing better on the Coulomb energy. A convenient description is through a parton construction $c_{i;\sigma} = b f_{i;\sigma}$ where the spinless slave boson b carries physical charge and f_σ is spin-1/2 neutral fermion. In the CFL phase, the boson is at filling $\nu = 1$ of a $C = 1$ band and can form a Fractional Chern insulator (Pfaffian state) with $\sigma_{xy} = \frac{e^2}{h}$, $\sigma_{xx} = 0$. Using the Ioffe-Larkin rule[57], we get the resistivity tensor of the physical electrons: $\rho^c = \rho^f + \rho^b$. In the clean limit, $\rho^b = \begin{pmatrix} 0 & -\frac{h}{e^2} \\ \frac{h}{e^2} & 0 \end{pmatrix}$ and $|\rho^f| \ll 1$ is metallic. Then we get $\rho_{xy}^c \sim \frac{h}{e^2} \gg \rho_{xx}^c \sim \rho_{xx}^f$. Then the Hall angle $\tan^{-1} \left(\frac{\rho_{xy}^c}{\rho_{xx}^c} \right)$ is close to, but strictly smaller, than 90° . More details on this CFL phase can be found in the sup-

plementary.

Thus the spin unpolarized composite Fermi liquid provides a concrete interesting intermediate coupling metallic state with a large Hall angle. This state will show SdH oscillations with a frequency that, in contrast to the partially spin polarized Fermi liquid, matches the band theory Fermi liquid. Other related novel states of matter can also be contemplated but we will leave their elaboration to the future.

Though the Hall angle in the experiments is large, it clearly does not precisely match the expectation of an ideal quantized anomalous Hall system or of the composite fermi liquid. This is possibly due both to the presence of disorder and to the presence of the quasi-periodic potential. In particular the quasiperiodic potential may produce nearly extended in-gap states which may reduce the Hall angle to close to 45° in the experiment. Finally we remark that in both the QAH and the CFL state the conduction is predominantly through the sample edge which will lead to non-local response consistent with experiments.

We now turn to the correlated insulator observed at $\nu = \frac{1}{2}$. While more exotic phases cannot be ruled out, the observed two fold degeneracy of the Landau fan[6] suggests a simple picture of a ferromagnetic insulator. Further, based on the experiment result[6] that the resistivity is enhanced with an out of plane magnetic field (which has a valley Zeeman coupling, see the supplementary), we suggest the $\nu = \frac{1}{2}$ insulator has an inter-valley-coherent order with $\tau_{x,y}$ or $\tau_{x,y}\vec{\sigma}$ valley polarization (see the supplementary). Energetically within a Hartree-Fock theory in momentum space such an IVC order is known to be favored when the anisotropy $\delta\xi(\mathbf{k}) = |\xi_+(\mathbf{k}) - \xi_-(\mathbf{k})|$ is large[7, 11, 54]. In the supplementary we show that $\tau_x\vec{\sigma}$ is selected by the inter-valley Hund's term breaking $U(2)_+ \times U(2)_-$ symmetry of separate spin and charge conservation of each valley down to $U(1)_{charge} \times U(1)_{valley} \times SU(2)_{spin}$. An in-plane magnetic field H_x further favors $\tau_x\sigma_{y,z}$.

In conclusion, we described several aspects of the physics of Magic Angle Twisted Bilayer Graphene aligned with a h-BN substrate. The C_2 breaking due to alignment with h-BN gaps the Dirac points of TBG, and further renders the conduction and valence bands with Chern numbers $C = \pm 1$. This suggests a natural explanation of the recent observation[6] of a large anomalous Hall effect at $3/4$ -filling of the conduction band, as a spontaneously spin-valley polarized ferromagnetic Chern insulator. Energetically such a state is natural when the Coulomb interaction is strong compared to the bandwidth. At intermediate coupling, other more novel states with a large anomalous but unquantized Hall effect, are possible. The concrete example we discussed - a spin unpolarized composite fermi liquid - may provide an alternate explanation of the data. We constructed a lattice extended Hubbard model for TBG/h-BN which may be

useful for future numerical explorations of intermediate coupling phases. Further this model could also provide an effective model for TBG if C_2T is spontaneously broken.

We thank A. Sharpe and D. Goldhaber-Gordon for sharing their data prior to publication, and for very useful comments. Our discussion overlaps that of an upcoming paper by N. Bultinck, S. Chatterjee, and M. Zaletel, also on TBG/h-BN. We thank M. Zaletel for inspiring conversations about this and related problems. This work was supported by NSF grant DMR-1608505, and partially through a Simons Investigator Award from the Simons Foundation to Senthil Todadri.

-
- [1] E. M. Spanton, A. A. Zibrov, H. Zhou, T. Taniguchi, K. Watanabe, M. P. Zaletel, and A. F. Young, *Science* **360**, 62 (2018).
- [2] Y. Cao, V. Fatemi, A. Demir, S. Fang, S. L. Tomarken, J. Y. Luo, J. D. Sanchez-Yamagishi, K. Watanabe, T. Taniguchi, E. Kaxiras, *et al.*, *Nature* **556**, 80 (2018).
- [3] Y. Cao, V. Fatemi, S. Fang, K. Watanabe, T. Taniguchi, E. Kaxiras, and P. Jarillo-Herrero, *Nature* **556**, 43 (2018).
- [4] G. Chen, L. Jiang, S. Wu, B. Lv, H. Li, K. Watanabe, T. Taniguchi, Z. Shi, Y. Zhang, and F. Wang, arXiv preprint arXiv:1803.01985 (2018).
- [5] M. Yankowitz, S. Chen, H. Polshyn, K. Watanabe, T. Taniguchi, D. Graf, A. F. Young, and C. R. Dean, arXiv preprint arXiv:1808.07865 (2018).
- [6] A. L. Sharpe, E. J. Fox, A. W. Barnard, J. Finney, K. Watanabe, T. Taniguchi, M. A. Kastner, and D. Goldhaber-Gordon, arXiv preprint arXiv:1901.03520 (2019).
- [7] Y.-H. Zhang, D. Mao, Y. Cao, P. Jarillo-Herrero, and T. Senthil, arXiv preprint arXiv:1805.08232 (2018).
- [8] M. Xie and A. H. MacDonald, arXiv preprint arXiv:1812.04213 (2018).
- [9] J. Jung, A. Raoux, Z. Qiao, and A. H. MacDonald, *Physical Review B* **89**, 205414 (2014).
- [10] C. Xu and L. Balents, arXiv preprint arXiv:1803.08057 (2018).
- [11] H. C. Po, L. Zou, A. Vishwanath, and T. Senthil, *Phys. Rev. X* **8**, 031089 (2018).
- [12] M. Koshino, N. F. Yuan, T. Koretsune, M. Ochi, K. Kuroki, and L. Fu, *Physical Review X* **8**, 031087 (2018).
- [13] J. Kang and O. Vafek, arXiv preprint arXiv:1805.04918 (2018).
- [14] N. F. Yuan and L. Fu, arXiv preprint arXiv:1803.09699 (2018).
- [15] J. F. Dodaro, S. A. Kivelson, Y. Schattner, X.-Q. Sun, and C. Wang, arXiv preprint arXiv:1804.03162 (2018).
- [16] M. Ochi, M. Koshino, and K. Kuroki, arXiv preprint arXiv:1805.09606 (2018).
- [17] H. Isobe, N. F. Yuan, and L. Fu, *Physical Review X* **8**, 041041 (2018).
- [18] B. Padhi, C. Setty, and P. W. Phillips, *Nano letters* **18**, 6175 (2018).
- [19] J. Pizarro, M. Calderón, and E. Bascones, arXiv preprint arXiv:1805.07303 (2018).
- [20] J. Gonzalez and T. Stauber, arXiv preprint arXiv:1807.01275 (2018).
- [21] A. Thomson, S. Chatterjee, S. Sachdev, and M. S. Scheurer, *Physical Review B* **98**, 075109 (2018).
- [22] Y. Sherkunov and J. J. Betouras, *Physical Review B* **98**, 205151 (2018).
- [23] T. Huang, L. Zhang, and T. Ma, arXiv preprint arXiv:1804.06096 (2018).
- [24] D. M. Kennes, J. Lischner, and C. Karrasch, arXiv preprint arXiv:1805.06310 (2018).
- [25] C.-C. Liu, L.-D. Zhang, W.-Q. Chen, and F. Yang, *Physical review letters* **121**, 217001 (2018).
- [26] L. Rademaker and P. Mellado, arXiv preprint arXiv:1805.05294 (2018).
- [27] J. W. Venderbos and R. M. Fernandes, *Physical Review B* **98**, 245103 (2018).
- [28] H. Guo, X. Zhu, S. Feng, and R. T. Scalettar, arXiv preprint arXiv:1804.00159 (2018).
- [29] Y.-P. Lin and R. M. Nandkishore, *Physical Review B* **98**, 214521 (2018).
- [30] L. Zhang, arXiv preprint arXiv:1804.09047 (2018).
- [31] M. Fidrysiak, M. Zegrodnik, and J. Spalek, *Physical Review B* **98**, 085436 (2018).
- [32] B. Roy and V. Juricic, arXiv preprint arXiv:1803.11190 (2018).
- [33] Y. Su and S.-Z. Lin, *Physical Review B* **98**, 195101 (2018).
- [34] S. Ray and T. Das, arXiv preprint arXiv:1804.09674 (2018).
- [35] L. Zou, H. C. Po, A. Vishwanath, and T. Senthil, arXiv preprint arXiv:1806.07873 (2018).
- [36] H. C. Po, L. Zou, T. Senthil, and A. Vishwanath, arXiv preprint arXiv:1808.02482 (2018).
- [37] Q. Tang, L. Yang, D. Wang, F. Zhang, and Q. Wang, arXiv preprint arXiv:1809.06772 (2018).
- [38] Y.-Z. You and A. Vishwanath, arXiv preprint arXiv:1805.06867 (2018).
- [39] G. Baskaran, arXiv preprint arXiv:1804.00627 (2018).
- [40] T. J. Peltonen, R. Ojajärvi, and T. T. Heikkilä, arXiv preprint arXiv:1805.01039 (2018).
- [41] V. Y. Irkhin and Y. N. Skryabin, *JETP Letters* , 1 (2018).
- [42] F. Wu, A. MacDonald, and I. Martin, arXiv preprint arXiv:1805.08735 (2018).
- [43] S. Carr, S. Fang, P. Jarillo-Herrero, and E. Kaxiras, arXiv preprint arXiv:1806.05078 (2018).
- [44] F. Guinea and N. R. Walet, *Proceedings of the National Academy of Sciences* **115**, 13174 (2018).
- [45] B. Lian, F. Xie, and B. A. Bernevig, arXiv preprint arXiv:1811.11786 (2018).
- [46] B. Lian, Z. Wang, and B. A. Bernevig, arXiv preprint arXiv:1807.04382 (2018).
- [47] Z. Song, Z. Wang, W. Shi, G. Li, C. Fang, and B. A. Bernevig, arXiv preprint arXiv:1807.10676 (2018).
- [48] J. Ahn, S. Park, and B.-J. Yang, arXiv preprint arXiv:1808.05375 (2018).
- [49] E. Laksono, J. N. Leaw, A. Reaves, M. Singh, X. Wang, S. Adam, and X. Gu, *Solid State Communications* **282**, 38 (2018).
- [50] L. Chen, H.-Z. Li, and R.-S. Han, *Journal of Physics: Condensed Matter* **31**, 065601 (2018).
- [51] Z. Liu, Y. Li, and Y.-f. Yang, arXiv preprint arXiv:1901.00083 (2019).
- [52] R. Bistritzer and A. H. MacDonald, *Proceedings of the*

- National Academy of Sciences **108**, 12233 (2011).
- [53] D. Xiao, M.-C. Chang, and Q. Niu, Reviews of modern physics **82**, 1959 (2010).
- [54] Y.-H. Zhang and T. Senthil, arXiv preprint arXiv:1809.05110 (2018).
- [55] J. Kang and O. Vafek, arXiv preprint arXiv:1810.08642 (2018).
- [56] Note that as there is spin $SU(2)$ symmetry, spontaneous spin polarization will not lead to hysteresis; the valley polarization however is an Ising order parameter and hence hysteresis is expected.
- [57] L. Ioffe and A. Larkin, Physical Review B **39**, 8988 (1989).

Supplementary Material for “Twisted Bilayer Graphene Aligned with Hexagonal Boron Nitride: Anomalous Hall Effect and a Lattice Model”

BAND STRUCTURE CALCULATION

The continuum model for the TBG is[S52]

$$\begin{aligned}
 H_{TBG} = & \sum_{\alpha=t,b} \sum_{\mathbf{k}} \psi_{\alpha}^{\dagger}(\mathbf{k}) h_0^{\dagger} \psi_{\alpha}(\mathbf{k}) \\
 & + \sum_{\mathbf{k}, j=1,2,3} \left(\psi_t^{\dagger}(\mathbf{k} + \mathbf{Q}_j) T_j \psi_b(\mathbf{k}) + h.c. \right)
 \end{aligned} \tag{S1}$$

Here we focus on valley $+$. The other valley is related by time reversal transformation. ψ_{α} is a two component spinor in terms of A and B sublattice for each layer. h_0^{\dagger} is the standard Dirac Hamiltonian:

$$h_0^{\dagger} = k_x \mu_1 + k_y \mu_2 \tag{S2}$$

where μ_a is the Pauli matrix in the sublattice A, B space for the top layer or the bottom layer. $T_j, j = 1, 2, 3$ is the moiré term for the inter-layer coupling. $\mathbf{Q}_1 = R_{-\theta_M/2} \mathbf{K}_o - R_{\theta_M/2} \mathbf{K}_o$, where R_{θ} rotates a $2D$ vector by θ around the z direction. K_o is one of the corners of their original large Brillouin zone.

$$T_1 = w_0 - w_1 \mu_1 \tag{S3}$$

Q_2, Q_3 and T_2, T_3 are generated by C_3 symmetry: $\psi_{\alpha}(\mathbf{k}) \rightarrow e^{i\frac{2\pi}{3}\mu_3} \psi_{\alpha}(C_3 \mathbf{k})$.

We use the parameters $w_1 = 110$ meV and $\frac{w_0}{w_1} = 0.7$ [S12] to incorporate the lattice relaxation effects. This value of $\frac{w_0}{w_1}$ gives a hybridization gap around $30 - 40$ meV between the valence band and the band below for twist angle $\theta_M = 1.05^{\circ} - 1.20^{\circ}$, consistent with the experimental measurement[S2].

As argued in the main text, the aligned h-BN layer on the top provides a mass term for the top graphene layer:

$$H_{hBN} = M \sum_{\mathbf{k}} \psi_t^{\dagger}(\mathbf{k}) \mu_z \psi_t(\mathbf{k}) \tag{S4}$$

We then diagonalize $H_{TBG} + H_{hBN}$ from Eq. S1 and Eq. S4 and get the band structure shown in Fig.1 of the main text. Due to the twist angle θ_M , the original Dirac cone at K_o point for the top graphene layer is put at K' point of the Mini Brillouin Zone (MBZ) while the original Dirac cone at K_o for the bottom graphene layer is put at K point of the MBZ.

In the presence of the M term in the Eq. S4, the Dirac crossing is gapped at K' point even if we suppress the inter-layer coupling T_j to zero. With the inter-layer coupling T_j , the Dirac cone at K point is also gapped. The band gap at K' is around 10 meV while the band gap at K point is only 5 meV. Note that there is no symmetry relating K and K' . Also, the conduction and the valence bands are well separated from the other bands using $\frac{w_0}{w_1} = 0.7$, as shown in Fig. S1, and from each other. Thus the Chern numbers are well defined for both conduction and valence bands. We calculate the Chern number of each band following the same method used in Ref. S7. For the valley $+$, we find that the conduction and the valence bands have Chern numbers $C = 1$ and $C = -1$ respectively. Because of the time reversal symmetry, the other valley must have opposite Chern numbers.

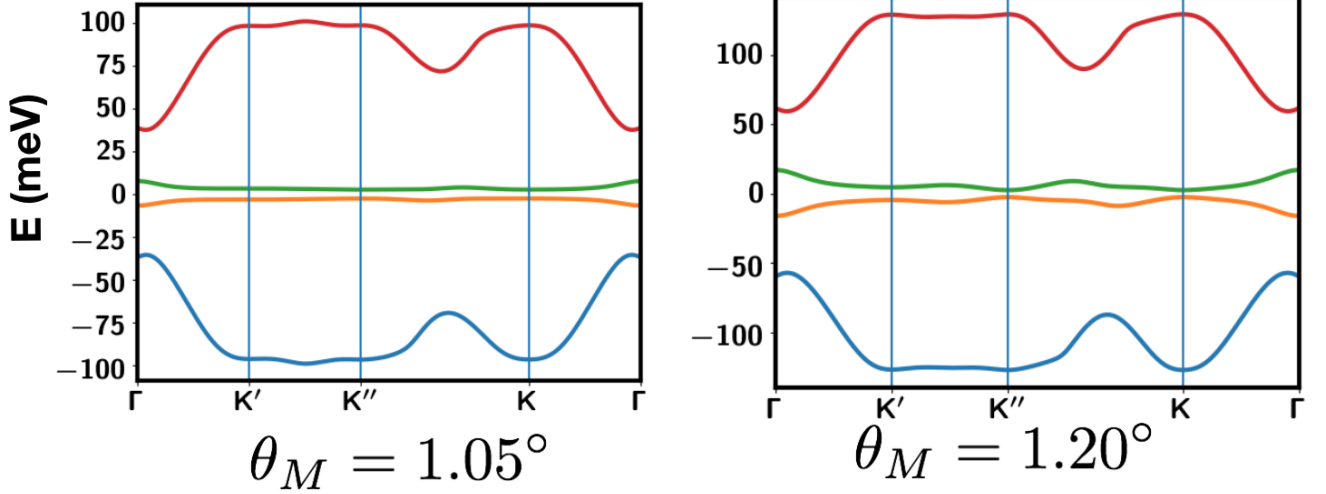


FIG. S1: Band structure for valley + of the TBG-h-BN system in the MBZ. The middle two bands are well separated from the other bands. The middle two bands have Chern numbers $C = 1$ and $C = -1$. We use $\frac{w_0}{w_1} = 0.7$ to incorporate the lattice relaxation effects.

Valley Zeeman Coupling

As discussed in the main text, the alignment of the h-BN gives a mass to the Dirac cones at K and K' point in the MBZ for each spin and each valley. As well known, massive Dirac fermion can have an out of plane magnetic moment, which is opposite for opposite valleys. Therefore there is a valley Zeeman coupling to the out of plane magnetic field:

$$H_v = -\frac{1}{2}\mu_B H \sum_{\mathbf{k}} g_v(\mathbf{k}) c^\dagger(\mathbf{k}) \tau_z c(\mathbf{k}) \quad (\text{S5})$$

with $g_v \sim \frac{1}{\Delta}$. We numerically calculated g_v for $\theta_M = 1.20^\circ$ and $M = 15$ meV. Indeed we find that close to the K and K' point, $g_v(K) \approx g_v(K') \approx 15$ for both the conduction and valence bands, which is one order of magnitude larger than the spin Zeeman coupling. Averaging over the whole MBZ, we have $\bar{g}_v \approx 4$ because the valley Zeeman coupling away from the K and K' points is small.

The valley Zeeman coupling provides a simple explanation of the observed[S6] reduction of the degeneracy in the Landau fan emanating from the neutrality point. Close to neutrality the Landau fan is from a Fermi pocket at K point for each flavor (The degeneracy between K and K' is lifted by the alignment of the h-BN layer). The large valley Zeeman splitting (1.5 meV for 1 Tesla) can reduce the degeneracy to only 2 (coming from spin).

LATTICE MODEL

The TBG system has a Wannier obstruction to construct a valley preserving and C_2T symmetric model[S11, S35, S36, S47, S48]. In the TBG-hBN, the C_2T is broken by the alignment to h-BN. As a result, there is no Wannier obstruction for a valley preserving lattice model. For each valley, the conduction and the valence bands have the opposite Chern numbers, we can build a lattice model by combining both bands. We constructed the Wannier orbitals following the standard projection methods[?]. The resulting lattice model is a modified "Haldane model" on a honeycomb lattice for each valley. However, the two lattice sublattice sites correspond to the AB and BA regions, while the density is concentrated on the AA regions. Therefore each Wannier orbital has the shape of a fidget spinner similar to Ref. S11.

Tight binding parameters

In Table. S1 we show tight binding parameters defined in the main text for two twist angles.

θ_M	m_0	t	t'_A	t'_B	t''	t'''_1	t'''_2
1.08°	1.36	1.22	$0.670e^{i0.366\pi}$	$0.731e^{-i0.657\pi}$	$0.801e^{-i0.685\pi}$	$0.123e^{-i0.48\pi}$	$0.355e^{-i0.411\pi}$
1.20°	0.076	3.056	$0.837e^{i0.56\pi}$	$0.828e^{-i0.469\pi}$	$2.062e^{-i0.54\pi}$	$0.915e^{-i0.337\pi}$	$0.815e^{-i0.434\pi}$

TABLE S1: Tight binding model parameters for the modified Haldane model in units of meV.

Quasi-Periodic Potential

We also need to add a quasi-periodic potential term from projecting the V_j term in Eq. 2 to the two orbitals.

$$H_{QP} = V_{QP} \sum_i \cos(\mathbf{Q}'_j \cdot \mathbf{R}_i) c_{i;a\sigma}^\dagger c_{i;a\sigma} \quad (\text{S6})$$

where we ignored the quasi-periodicity in the hopping terms for simplicity. The value of V_{QP} can be tuned by displacement field and we keep it as a free parameter.

$M \rightarrow 0$ Limit

For any finite M we can build a lattice model on a honeycomb lattice, as done in the main text. This process can be even extrapolated to the $M \rightarrow 0$ limit. How is this consistent with the Wannier obstruction at $M = 0$? In the following we try to resolve this puzzle. The Wannier obstruction at $M = 0$ is related to the C_2T symmetry and is therefore different from the intrinsic Wannier obstruction for the Chern band. Once C_2T breaking is allowed, an exponentially localized Wannier orbital is possible and we can actually recover the gapless Dirac crossing with finite range of hopping, like $R < 7$. This process is conceptually similar to the Wannier construction process by ignoring the $U(1)$ valley symmetry in Ref. S11.

In this process, the lattice model contains C_2T breaking terms even in the $M \rightarrow 0$ limit. The typical C_2T breaking term is the next-nearest neighbor hopping $t'_A \approx -t'_B = t'$. As shown in Fig. S2, when the external C_2T breaking term M is large, the lattice model has a C_2T breaking term $t' \propto M$. When M is small, the C_2T breaking term in our lattice model is obviously overestimated. With enough range of hopping, we can still reduce the band gap in the lattice model to be proportional to M at $M \rightarrow 0$ limit. This means that the lattice model with enough range of hopping has a hidden non-local C_2T symmetry. If one can keep all these non-local terms in the lattice model, one can still get the correct result of Dirac crossings between valence and conduction bands. However, the purpose of a lattice model is to do a useful approximation. Such a lattice model with a non-local C_2T symmetry(see, eg, Ref. [S55]) is dangerous because it is not clear how to do approximate calculations that maintain this symmetry. (Similarly, if one does not insist on a local representation of the $U(1)_{valley}$ symmetry, a lattice model is also possible in the $M \rightarrow 0$ limit, as explicitly done in Ref. S11). Thus a useful lattice model that keeps just the states from the active bands is possible only for the large M regime, i.e. when h-BN is aligned.

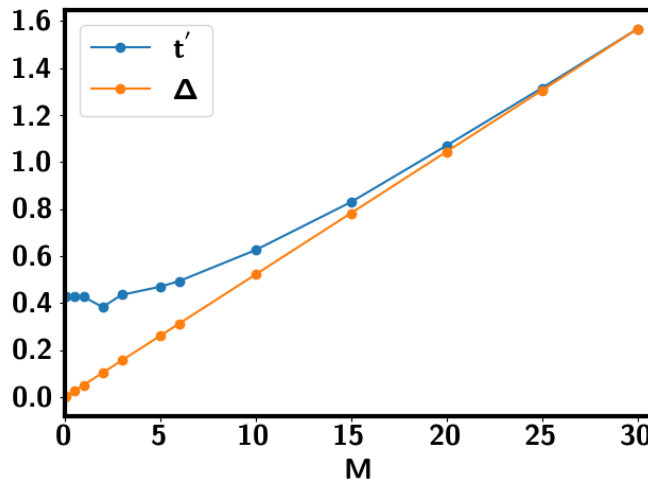


FIG. S2: The C_2T breaking term in the lattice model t' and the band gap Δ with M . As $M \rightarrow 0$, the lattice model does not have obvious C_2T symmetry.

FERROMAGNETIC INSULATOR AT $\nu = \frac{1}{2}$

At $\nu = \frac{1}{2}$, there is exactly one hole at each honeycomb lattice site. Therefore a strong coupling approach for $U \gg t, t'$ with inter-site Hund's term favors a simple insulator which puts a spin-valley polarized hole at each site[S54, S55]. Either τ_z or τ_x valley polarization is selected depending on the competition between the interaction and the kinetic term[S54]. However, this phase leaves both the conduction and valence band of one flavor empty, which costs kinetic energy. Therefore, for the experimentally relevant $U \sim W$ regime, the strong coupling approach is also not appropriate at $\nu = \frac{1}{2}$.

For $U \sim W$, a more natural FM order is one where only the conduction bands of two flavors are pushed up while the other two conduction bands are fully filled. This is described by the order parameter $c^\dagger \tau_a \sigma_b c$ where c is the electron destruction operator for the conduction band (we suppressed the spin-valley index). τ^a are Pauli matrices in valley space and σ^a are spin Pauli matrices.

We only consider FM order without momentum dependence (*i.e.* the particle-hole pair that forms the order parameter has zero internal momentum). There are 15 such order parameters corresponding to $\tau^a, \sigma^a, \tau^a \sigma^b$. Our system has an approximate symmetry $U(2)_+ \times U(2)_-$ [S7, S11] generated by $\vec{\sigma}, \tau_z \vec{\sigma}, \tau_z$ and the total charge. For any particle-hole order $\psi^\dagger A \psi$ with A a 4×4 matrix, another order is degenerate from the spin-valley rotation: $A \rightarrow U A U^\dagger$ where $U \in U(2)_+ \times U(2)_-$. It is then easy to verify that the 15 FM orders can be grouped to three classes: (1) τ_z ; (2) $\tau_z \vec{\sigma}, \vec{\sigma}$; (3) $\tau_{x,y}, \tau_{x,y} \vec{\sigma}$. We can try to decide which of these distinct FM orders is selected by the anisotropies in the Hamiltonian based on a simple Hartree-Fock calculation. For fully polarized states with τ^z or $\tau^z \vec{\sigma}$ ordering, the Hartree-Fock energies are readily seen to be the same. Thus it suffices to compare τ^z and $\tau^{x,y}$ ordering. As argued in previous papers[S7, S11], within such a Hartree-Fock calculation, either τ^z or $\tau^{x,y}$ ordering wins depending on the bandwidth. The flat band limit prefers τ^z while for wider bands it is possible to stabilize $\tau^{x,y}$. A further selection within each group of orders related by $U(2)_+ \times U(2)_-$ occurs through a weak inter-valley Hund's interaction that locks spins in the two valleys together.

We therefore proceed phenomenologically, and ask which such order is consistent with results from experiments[S6] at $\nu = \frac{1}{2}$. First τ_z can be ruled out because of the absence of anomalous Hall effect at this filling. Another important information in the experiment is that the resistivity increases with out of plane magnetic field. As discussed in the previous section, the dominant effect of an out of plane magnetic field is a valley Zeeman coupling $-g_v \mu_B H_z \frac{\tau_z}{2}$. For the $\vec{\sigma}$ and the $\tau_z \vec{\sigma}$ order, one valley + and one valley - band are filled while the other two valley + and - bands are pushed to higher energy with a charge gap $\Delta_c = \Phi - W$ (Φ is the strength of the splitting of the band due to the order parameter. We assume Φ is larger than the bandwidth W so as to get an insulator). With a valley Zeeman coupling, the charge gap Δ_c decreases: $\Delta_c(H_z) = \Delta_c(0) - g_v \mu_B H$, inconsistent with the experiment.

The only FM order consistent with the experiment is the $\tau_{x,y}$ or $\tau_{x,y} \vec{\sigma}$. They are degenerate so long as there is $U(2)_+ \times U(2)_-$ symmetry. However this degeneracy is broken by a weak inter-valley exchange interaction or by an external magnetic field. Let us first consider the former. The pertinent inter-valley interaction arises microscopically

from large momentum transfer contribution to the density-density repulsion. Further, for clarity, we initially present the argument in a form appropriate for a topologically trivial band and later argue that the conclusions remain unchanged for a Chern band - this amounts to initially ignoring form factors associated with Bloch wavefunctions in the interaction. Therefore we consider

$$H_J = \frac{g}{N} \sum_{\sigma_1 \sigma_2} \sum_{\mathbf{k}_1, \mathbf{k}_2, \mathbf{q}} c_{+\sigma_1}^\dagger(\mathbf{k}_1 + \mathbf{q}) c_{-\sigma_1}(\mathbf{k}_1) c_{-\sigma_2}^\dagger(\mathbf{k}_2 - \mathbf{q}) c_{+\sigma_2}(\mathbf{k}_2) \quad (\text{S7})$$

where $g = V(2K_o)$ where K_o is a large momentum in the original large Brillouin zone. N is the number of moiré sites. Here $c_{a\sigma}(\mathbf{k})$ is the creation operator of the conduction band. The above term is equivalent to an inter-valley Hund's term [S7]:

$$H_J = -\frac{g}{N} \sum_{\mathbf{q}} \mathbf{S}_+(\mathbf{q}) \cdot \mathbf{S}_(-\mathbf{q}) - \frac{g}{2N} \sum_{\mathbf{q}} n_+(\mathbf{q}) n_-(-\mathbf{q}) \quad (\text{S8})$$

where $\mathbf{S}_a(\mathbf{q}) = \sum_{\mathbf{k}} c_a^\dagger(\mathbf{k} + \mathbf{q}) \frac{\sigma}{2} c_a(\mathbf{k})$. It is more transparent to work with this form of Eq. S7.

For simplicity we consider the maximally polarized τ_x or $\tau_x \sigma_z$ orders. We label S and A as the valley polarization corresponding to 1 and -1 of τ_x . Then for τ_x ordering the two filled conduction bands are $S \uparrow, S \downarrow$. For $\tau_x \sigma_z$ ordering, the two filled bands are $S \uparrow, A \downarrow$. We calculate $\langle H_J \rangle$ using Wick theorem. From $c_{\pm, \sigma}(\mathbf{k}) = \frac{1}{\sqrt{2}}(c_{S\sigma}(\mathbf{k}) \pm c_{A\sigma}(\mathbf{k}))$ and $\langle c_S^\dagger(\mathbf{k}) c_A(\mathbf{k}) \rangle = 0$, we have $\langle c_{+\sigma}^\dagger(\mathbf{k}) c_{+\sigma}(\mathbf{k}) \rangle = \langle c_{-\sigma}^\dagger(\mathbf{k}) c_{-\sigma}(\mathbf{k}) \rangle = \frac{1}{2} \left(\langle c_{S\sigma}^\dagger(\mathbf{k}) c_{S\sigma}(\mathbf{k}) \rangle + \langle c_{A\sigma}^\dagger(\mathbf{k}) c_{A\sigma}(\mathbf{k}) \rangle \right)$ and $\langle c_{+\sigma}^\dagger(\mathbf{k}) c_{-\sigma}(\mathbf{k}) \rangle = \langle c_{-\sigma}^\dagger(\mathbf{k}) c_{+\sigma}(\mathbf{k}) \rangle = \frac{1}{2} \left(\langle c_{S\sigma}^\dagger(\mathbf{k}) c_{S\sigma}(\mathbf{k}) \rangle - \langle c_{A\sigma}^\dagger(\mathbf{k}) c_{A\sigma}(\mathbf{k}) \rangle \right)$.

Labeling $n_{p, \sigma}(\mathbf{k}) = \frac{1}{2} \langle c_{S\sigma}^\dagger(\mathbf{k}) c_{S\sigma}(\mathbf{k}) + c_{A\sigma}^\dagger(\mathbf{k}) c_{A\sigma}(\mathbf{k}) \rangle$ and $n_{m, \sigma}(\mathbf{k}) = \frac{1}{2} \langle c_{S\sigma}^\dagger(\mathbf{k}) c_{S\sigma}(\mathbf{k}) - c_{A\sigma}^\dagger(\mathbf{k}) c_{A\sigma}(\mathbf{k}) \rangle$, we have

$$\begin{aligned} \langle H_J \rangle &= -\frac{g}{N} \sum_{\sigma} \sum_{\mathbf{k}, \mathbf{q}} \langle c_{+\sigma}^\dagger(\mathbf{k} + \mathbf{q}) c_{+\sigma}(\mathbf{k} + \mathbf{q}) \rangle \langle c_{-\sigma}^\dagger(\mathbf{k}_1) c_{-\sigma}(\mathbf{k}_1) \rangle + \frac{g}{N} \sum_{\sigma_1 \sigma_2} \sum_{\mathbf{k}_1, \mathbf{k}_2} \langle c_{+\sigma_1}^\dagger(\mathbf{k}_1) c_{-\sigma_1}(\mathbf{k}_1) \rangle \langle c_{-\sigma_2}^\dagger(\mathbf{k}_2) c_{+\sigma_2}(\mathbf{k}_2) \rangle \\ &= -\frac{g}{N} \sum_{\sigma} \sum_{\mathbf{k}_1, \mathbf{k}_2} n_{p\sigma}(\mathbf{k}_1) n_{p\sigma}(\mathbf{k}_2) + \frac{g}{N} \sum_{\sigma_1 \sigma_2} \sum_{\mathbf{k}_1, \mathbf{k}_2} n_{m\sigma_1}(\mathbf{k}_1) n_{m\sigma_2}(\mathbf{k}_2) \\ &= -\frac{g}{N} \sum_{\sigma} \sum_{\mathbf{k}_1, \mathbf{k}_2} n_{p\sigma}(\mathbf{k}_1) n_{p\sigma}(\mathbf{k}_2) + \frac{g}{N} \sum_{\mathbf{k}_1, \mathbf{k}_2} n_m(\mathbf{k}_1) n_m(\mathbf{k}_2) \end{aligned} \quad (\text{S9})$$

where $n_m(\mathbf{k}) = n_{m\uparrow}(\mathbf{k}) + n_{m\downarrow}(\mathbf{k})$ is the difference between the occupation number of the S band and the A band.

For τ_x and $\tau_x \sigma_z$ order, the first term is the same: $-2gN$. For the second term, τ_x order contributes $4gN$ while $\tau_x \sigma_z$ order contributes zero. Therefore we conclude that $\tau_x \vec{\sigma}$ is selected by the term breaking $U(2)_+ \times U(2)_-$ down to $U(1)_c \times U(1)_v \times SU(2)_s$.

We now argue the same conclusion holds for a Chern band; then we cannot fix a smooth gauge for $c(\mathbf{k})$. Instead, we need to use $c_{a\sigma}(\mathbf{k}) \rightarrow e^{-i\theta_a(\mathbf{k})} c_{a\sigma}(\mathbf{k})$ in the interaction in Eq. S7. In the Hattree-Fock calculation, these additional form factors $e^{-i\theta_a(\mathbf{k})}$ cancel in the first term in Eq. S9. The form factors need to enter in the second term. However, we also need to add the same form factors in the eigenstate of τ_x . We have $c_{\pm, \sigma}(\mathbf{k}) = e^{i\theta_{\pm}(\mathbf{k})} \frac{1}{\sqrt{2}}(c_{S\sigma}(\mathbf{k}) \pm c_{A\sigma}(\mathbf{k}))$. Then the form factor $e^{-i\theta_a(\mathbf{k})}$ will also be cancelled in the second term of Eq. S9 and we can express it in terms of the gauge invariant term $c_S^\dagger(\mathbf{k}) c_S(\mathbf{k})$ and $c_A^\dagger(\mathbf{k}) c_A(\mathbf{k})$. Finally we reach the conclusion that for the Chern band, $\tau_x \vec{\sigma}$ is also selected.

In the above calculation, we assume maximally polarized τ_x or $\tau_x \vec{\sigma}$ order. In reality the IVC order may not be maximally polarized. While we do not have a proof for this more complicated case, the above analysis suggests that $\tau_x \vec{\sigma}$ order may also be selected.

In the presence of an out of plane magnetic field, the mean field Hamiltonian (assuming $\tau_x \sigma_z$ order) is:

$$H_M = - \sum_{\mathbf{k}} c^\dagger(\mathbf{k}) \left(\frac{\Phi}{2} \tau_x \sigma_z + \frac{1}{2} g_v(\mathbf{k}) \mu_B H_z \tau_z \right) \psi_c(\mathbf{k}) \quad (\text{S10})$$

Because τ_x anti-commutes with τ_z , the charge gap in the insulator is $\Delta_c(H_z) = \sqrt{\Phi^2 + g_v^2 \mu_B^2 H_z^2} - W$. If, as is reasonable, Φ has only a weak dependence on H_z , we conclude that the charge gap Δ_c can be greatly enhanced by the valley Zeeman field given that g_v is large (around 15 close to the K point), in agreement with what is measured. This conclusion does not depend on the detailed selection between τ_x and $\tau_x \vec{\sigma}$ discussed above.

The response to the in-plane magnetic field H_x (assuming it couples predominantly to the spin) however depends on whether τ_x or $\tau_x\vec{\sigma}$ is selected. Such a field can further split the energy degeneracy among $\tau_x\vec{\sigma}$. Because there is no spin magnetization, the field energy at first order of perturbation vanishes. For the second order perturbation, $\tau_x\sigma_{y,z}$ order can have a negative energy correction because $\tau_x\sigma_{y,z}$ anti-commutes with σ_x . Therefore in-plane magnetic field favors $\tau_x\sigma_{y,z}$. The splitting is of order $\frac{g_s^2\mu_B^2 H_x^2}{\Phi}$ and therefore is small.

SPINFUL COMPOSITE FERMION LIQUID

We give theoretical descriptions of several spinful CFL phases for the filling $\nu_T = \frac{1}{2} + \frac{1}{2}$ of the spinful $C = 1$ Chern band. As discussed in the main text, in the strict flat band limit, the simple ferromagnetic insulator will win. But the states discussed in this Appendix may be competitive once band dispersion becomes significant, i.e, for intermediate coupling $U \sim W$.

We do a slave-boson parton construction $c_{i;\sigma} = bf_{i;\sigma}$ (We can also do a slave fermion parton, which leads to a "quantum Hall spin liquid" insulator mentioned briefly at the end of this section.). b is a spinless boson which carries the physical charge while f_σ is a neutral spin-1/2 fermion. We have filling $n_b = 1$ and $\sum_\sigma n_{f;\sigma} = 1$. Besides, b and f need to couple to an internal $U(1)$ gauge field a with opposite charges.

In this parton construction we can access different phases by putting b and f in different phases. For the fermion f , the most natural ansatz is just a spin unpolarized state that with a fermi surface for each spin component. The spinless boson at $\nu = 1$ of a $C = 1$ Chern band can be either a Pfaffian state or itself form a Composite Fermi Liquid phase. For simplicity and because it is somewhat more familiar, here we focus on the former case. Then the boson has a quantum Hall effect with $\sigma_{xy}^b = \frac{e^2}{h}$. Such a phase has Ising anyons and the low energy effective theory is denoted $(U(1)_4 \times Ising)/Z_2$. In our case we need to further couple b to the internal gauge field a . For the purpose of the charge response of the microscopic electron, we can ignore the non-abelian Ising part and just write down the response of the slave boson b to the gauge field $A - a$ it couples to (A is the external probe electromagnetic gauge field). This is just a Chern-Simons term $\frac{1}{4\pi}(A - a)d(A - a)$. The low energy theory for the microscopic electron c is

$$L = \sum_\sigma L[f_\sigma, a] + \frac{1}{4\pi}ada - \frac{1}{2\pi}Ada + \frac{1}{4\pi}AdA + \dots \quad (S11)$$

This action resembles that of the standard Halperin-Lee-Read theory for the half filled Landau level[?]. However, for this state other terms need to be included to describe the Ising anyon of the slave boson though we will not explicitly write them here. For discussing low energy electrical transport the action above which describes the Fermi surfaces and the gauge field a is sufficient. In this sense, this CFL phase should have essentially the same properties as the conventional CFL phase. Close to the edge however, a neutral majorana mode may be present unlike the conventional composite fermi liquid.

From the Ioffe-Larkin rule[S57], the resistivity tensor of the original electron is

$$\rho^c = \rho^f + \rho^b \quad (S12)$$

Therefore we have:

$$\rho^c = \rho^f + \begin{pmatrix} 0 & -\frac{h}{e^2} \\ \frac{h}{e^2} & 0 \end{pmatrix} \quad (S13)$$

In the clean limit, ρ^f behaves like a metal and thus $|\rho^f| \ll \frac{h}{e^2}$. Therefore $\rho_{xy}^c \approx \frac{h}{e^2} \gg \rho_{xx}^c = \rho_{xx}^f$. Thus this phase has a large Hall angle, together with non-zero bulk dissipation.

Finally, we point out that the above CFL phase can go through a continuous phase transition by pairing of the composite fermions. In the simplest case, we just consider a spin singlet pairing $\langle f_\uparrow^\dagger f_\downarrow^\dagger \rangle \neq 0$, the resulting phase is an insulator with Hall conductivity $\sigma_{xy} = \frac{e^2}{h}$. The charge response is actually the same as the spin polarized Chern insulator. However, in this insulator the spin is in a singlet phase, and the elementary spin excitations are gapped spinons carrying spin 1/2, just like a Z_2 spin liquid. We dub this exotic insulator as "quantum Hall spin liquid". It is a non-trivial non-Abelian topological ordered phase. For example, the "vison" excitation in a conventional Z_2 spin liquid now carries 1/2 charge and is an Ising anyon, though it still has π mutual statistics with the gapped spinon. Details of this and other "quantum Hall spin liquid" phases will be discussed elsewhere.